

$$U(R) = - \frac{23 \alpha_A \alpha_B \hbar c}{4\pi R^4} \quad (30)$$

### V. SUMMARY

If one assumes that the universe contains random fluctuating classical radiation, then neutral polarizable particles are continually being polarized, and accordingly are continually emitting and absorbing radiation. In the asymptotic region where distances are large, only low-frequency field fluctuations will influence the attractions between neutral polarizable

particles. In this low-frequency domain, it is easy to calculate the dipole moments induced by the zero-point radiation and then to obtain the mutual forces between polarizable particles. Assuming a Lorentz invariant spectrum of classical fluctuating radiation with the scale set by Planck's constant, the results obtained for the attraction between a polarizable particle and a perfectly conducting wall, and between two neutral polarizable particles are in agreement with the quantum electrodynamic results of Casimir and Polder.

<sup>1</sup>H. B. G. Casimir and D. Polder, *Phys. Rev.* **73**, 360 (1948).

<sup>2</sup>F. London, *Z. Physik* **63**, 245 (1930); *Z. Physik. Chem.* **B11**, 222 (1930); *Trans. Faraday Soc.* **33**, 8 (1937).

<sup>3</sup>H. B. G. Casimir, *J. Chim. Phys.* **46**, 407 (1949).

<sup>4</sup>E. A. Power, *Introductory Quantum Electrodynamics* (Elsevier, New York, 1965).

<sup>5</sup>T. H. Boyer, *Phys. Rev.* **180**, 19 (1969).

<sup>6</sup>T. H. Boyer, *Phys. Rev.* **182**, 1374 (1969).

<sup>7</sup>T. H. Boyer, *Phys. Rev.* **186**, 1304 (1969).

<sup>8</sup>T. H. Boyer, *Phys. Rev. D* **1**, 1526 (1970).

<sup>9</sup>T. H. Boyer, *Phys. Rev. D* **1**, 2257 (1970).

<sup>10</sup>Essentially this same point of view appears in work by T. W. Marshall, *Proc. Roy. Soc. (London)* **A276**, 475 (1963); *Proc. Cambridge Phil. Soc.* **61**, 537 (1965); *Nuovo Cimento* **38**, 206 (1965).

<sup>11</sup>E. Nelson, *Phys. Rev.* **150**, 1079 (1966).

<sup>12</sup>T. H. Boyer (unpublished).

<sup>13</sup>M. Planck, *Theory of Heat Radiation* (Dover, New York, 1959).

<sup>14</sup>A. Einstein and L. Hopf, *Ann. Physik* **33**, 1105 (1910).

## Space-Charge-Controlled Diffusion in an Afterglow\*

M. A. Gusinow and R. A. Gerber

Sandia Laboratories, Albuquerque, New Mexico 87115

(Received 15 October 1971)

Calculations of space-charge-controlled diffusion of electrons and positive ions in an isothermal afterglow are presented. In particular, the transition from electron-ion ambipolar diffusion to free diffusion of the electrons and ions is investigated. The results are in qualitative agreement with the experiment of Gerber, Gusinow, and Gerardo insofar as predicting the general features of the transition from electron-ion ambipolar diffusion to free diffusion. In addition, the results substantiate the general behavior implicitly predicted by the more elaborate steady-state calculations of Allis and Rose.

### INTRODUCTION

This work reports calculations of space-charge-controlled diffusion of electrons and positive ions in an isothermal afterglow. In particular, the transition from electron-ion ambipolar diffusion to free diffusion of the electrons and ions is investigated.

Allis and Rose<sup>1</sup> (hereafter designated as AR) laid the foundations for this work in 1954 when they calculated the ionization rate necessary to maintain a steady-state discharge. Their result of interest here is the effective diffusion coefficients of electrons and (implicitly) positive ions as functions of the electron density in the discharge. In their conclusions it was pointed out that if the ionization fre-

quency in a steady-state discharge is associated with the electron loss rate in an afterglow, then the aforementioned effective diffusion coefficient should describe the electron loss rate in an afterglow.

To date there have been several attempts to test the AR theory.<sup>2,3</sup> These did not give quantitative agreement with theory. However, considering that the AR results were for hydrogen (in the steady state) and the experiments used helium<sup>2</sup> and neon<sup>3</sup> this is not surprising.

There have been many experiments in which a mass analyzer has been used to measure the ion decay rate (inferred from the ion wall current) during an afterglow. In this work we are concerned primarily with the experiments of Gerber *et al.*<sup>4</sup>

In those experiments the authors observed the transition from electron-positive ion ambipolar diffusion to free diffusion of the positive ions. The transition was evidenced by several decades of ion current for which the ion decay rate was faster than the rate of ambipolar diffusion. It was shown in the same work that the AR theory predicted this general type of behavior. In fact, the calculations of Cohen and Kruskal<sup>5</sup> as well as those of Kregel<sup>6</sup> also predict this behavior, although it is much easier to see this in the work of AR.

The main point of this work is to present explicit calculations of the electron and positive ion decay in an isothermal afterglow along with the ion and electron wall currents. Decay curves are presented which have as a parameter the ratio of the electron to positive ion diffusion coefficients. Due to numerical difficulties in solving the equations, an excessive amount of computer time is required to obtain calculations for realistic positive ions (that is, high ratios of electron to ion diffusion coefficients) and hence, only three types of ions are calculated, and limits on ion behavior are discussed.

#### CALCULATIONS

For an isothermal afterglow confined within an infinite parallel plane geometry, the equations that are to be solved in one dimension are the continuity equations for the electrons and ions and the Poisson equation for the self-consistent electric field:

$$\frac{\partial P}{\partial t} = D_+ \frac{\partial^2 P}{\partial x^2} - \mu_+ \frac{\partial}{\partial x} (PE), \quad (1)$$

$$\frac{\partial N}{\partial t} = D_- \frac{\partial^2 N}{\partial x^2} + \mu_- \frac{\partial}{\partial x} (NE), \quad (2)$$

$$\frac{\partial E}{\partial x} = \frac{e}{\epsilon_0} (P - N), \quad (3)$$

where  $P$  and  $N$  are the ion and electron densities in particles/m<sup>3</sup>,  $E$  is the magnitude of the space-charge electric field in V/m,  $\mu$  and  $D$  are the relevant species mobilities and diffusion coefficients, and  $e/\epsilon_0 = 1.809 \times 10^{-10}$  V m. It is pertinent to normalize the above equations as follows:

$$\frac{\partial p}{\partial \tau} = \frac{\partial^2 p}{\partial \rho^2} - \frac{\partial}{\partial \rho} (p \mathcal{E}), \quad (1')$$

$$\frac{\partial n}{\partial \tau} = s \frac{\partial^2 n}{\partial \rho^2} + s \frac{\partial}{\partial \rho} (n \mathcal{E}), \quad (2')$$

$$\mathcal{E} = \frac{e}{\epsilon_0} \frac{\pi^2}{4} \int_0^\rho (p - n) d\rho'. \quad (3')$$

Here  $p = (\mu\Lambda^2/D)P$ ,  $n = (\mu\Lambda^2/D)N$ ,  $s = D_-/D_+$ ,  $\tau = t/(L^2/D_+)$ ,  $\rho = x/L$ , and  $\Lambda = (2/\pi)L$ , where  $2L$  is the spacing of the parallel plate container. The quantity  $D/\mu$  is the ratio of the diffusion and mobility

coefficients for the electrons or ions and by the Einstein relation is equal to  $kT/e$  for an isothermal plasma. The results presented in this work are to be compared with those of Ref. 1. The quantities to be compared are the effective diffusion coefficients of the central electron and ion densities. In Ref. 1 these diffusion coefficients are presented as a function of  $N_0\Lambda^2\mu/D$ , while the calculations utilize a normalized (and dimensionless) density of  $N_0\Lambda^2\mu e/D\epsilon_0$ . Since Refs. 1 and 4 present the pertinent calculations as a function of the former normalized density, we have chosen to compute densities using the normalization factor  $D/\Lambda^2\mu$  even though this gives our densities the units of (Vm)<sup>-1</sup>. All currents will be normalized to  $(D_+/\Lambda^2L)(kT/e)$ . The electric field will be measured in units of  $(kT/e)/L$ . Notice that  $N\mu\Lambda^2/D = (\epsilon_0/\epsilon)(\Lambda/\Lambda_D)^2$ , where  $\Lambda_D$  is the electron shielding distance.

In using these equations to describe an isothermal afterglow, there are a number of assumptions: (i) The pressure of the neutral gas is high enough to ensure that the mean free paths are smaller than all relevant dimensions including the wall sheath. Consequently, the mean particle motions are determined by diffusion and mobility. This implies that the drift energy of each species should be small compared with its thermal energy. The statement concerning the sheath is necessary because in the sheath there exists a non-negligible space-charge electric field. If this field varies significantly over a mean free path, then a local relationship between the drift velocity and electric field does not exist. One must then resort to kinetic theory in much the same fashion as when calculating the anomalous skin depth in plasmas and metals.<sup>7,8</sup> (ii) The transport equations have been truncated after the first moment and hence the energy equation is not used. Inertia effects have been ignored. These effects have been considered to some degree by Persson<sup>9</sup> and Shimony and Cahn.<sup>10</sup> In not writing an energy-balance equation, it has been assumed that the electron and ion energies are uniform and equal throughout the medium. This clearly is inconsistent with the fact that the ions get accelerated in the sheath region and hence acquire a net drift velocity in crossing to the wall from the plasma volume. This may cause an error in considering sheath formation. (iii) The boundary conditions are that the electron and ion densities are zero at the wall and that  $\rho = 0$  is a center of symmetry such that all space derivatives are zero there.

These approximations are expected to have their largest effect near the onset of the transition when the sheath is thin. Nevertheless, it is meaningful to solve the set of equations (1')–(3') because the basic physical phenomenon causing the transition is contained in the nonlinear interaction between the charged-particle densities and the space-charge

electric field.

The equations were solved for  $p$ ,  $n$ , and  $\mathcal{E}$  as a function of  $\rho$  and  $\tau$  by finite difference methods using the alternating-direction implicit method.<sup>11,12</sup> For  $s=32$ , the cavity length was divided into 300 space zones and a time step of  $10^{-4}$  was used; for  $s=100$ , 500 space zones were used with a time step of  $2.5 \times 10^{-5}$ . The above space and time increments were chosen because changing them (increasing the number of space zones and decreasing the time steps) caused a maximum change in calculated values of less than 1%. For  $s=32$ , 6 min of CDC 6600 computer time was required; for  $s=100$ , 66 min were required. The case of  $s=\infty$  was calculated by forcing the electron density to be zero everywhere. This is the asymptotic case in that the space-charge field is due totally to the ion density and must be an upper bound insofar as the volume electric field and wall potential are concerned.

### RESULTS

Figure 1 illustrates the time dependence of the central ( $\rho=0$ ) electron and ion densities for  $s=32$ . At the early times shown in Fig. 1, the electrons and ions decay together at a rate about 24% in excess of the ambipolar rate (at this time  $\Lambda_D \approx 0.1\Lambda$ ).

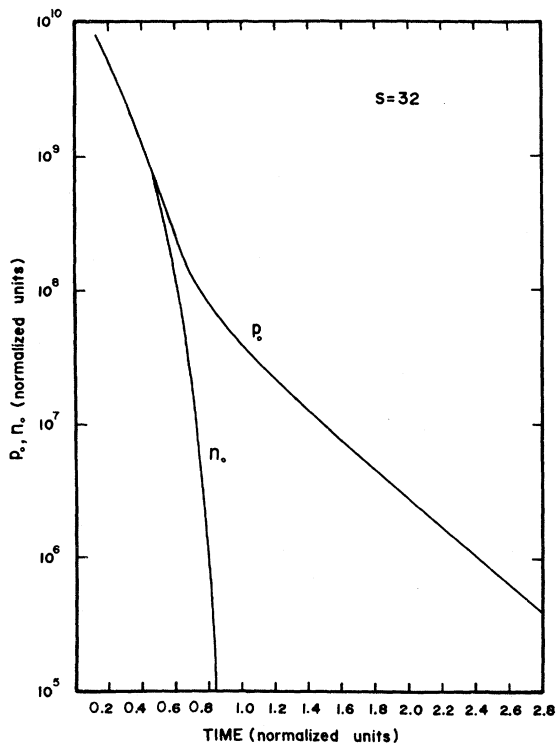


FIG. 1. The normalized central ( $\rho=0$ ) electron and ion densities  $n_0$  and  $p_0$  as a function of normalized time for  $s=32$ .

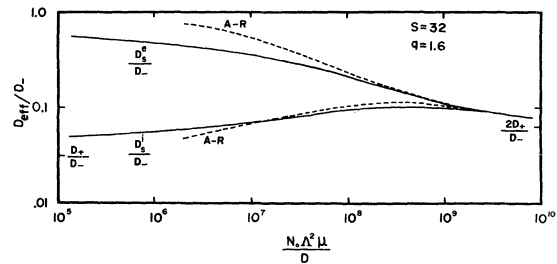


FIG. 2. The effective diffusion coefficient/ $D_+$  for the central electron and ion densities  $n_0$  and  $p_0$  as a function of  $N_0\Lambda^2\mu/D$  for  $s=32$ . The dashed curves were taken from the calculations presented in Ref. 1.

As the transition progresses, the electrons begin a very rapid approach to their free diffusion rate. The ions decay at a rate in excess of the ambipolar rate for several decades and then the ion decay rate decreases and finally approaches the free diffusion rate. It is during this transition period that the central space-charge density increases above its ambipolar value as shown in Fig. 6 of Ref. 1. This increase in central space-charge density manifests itself in a space-charge electric field larger than the ambipolar field (as shown in Fig. 4) with the result that the effective diffusion coefficient of the ions is increased above the ambipolar value. The effective diffusion coefficients of the central electron and ion densities are defined in Eqs. (4a) and (4b):

$$D_s^e = - \frac{\Lambda^2}{N} \frac{\partial N}{\partial t} \Big|_{x=0} = - \frac{4D_+}{\pi^2} \frac{1}{n} \frac{\partial n}{\partial \tau} \Big|_{\rho=0}, \quad (4a)$$

$$D_s^i = - \frac{\Lambda^2}{P} \frac{\partial P}{\partial t} \Big|_{x=0} = - \frac{4D_+}{\pi^2} \frac{1}{p} \frac{\partial p}{\partial \tau} \Big|_{\rho=0}. \quad (4b)$$

The effective diffusion coefficients for the central densities are shown in Fig. 2 as a function of  $N_0\Lambda^2\mu/D$ , where  $N_0$  is the central electron density. For comparison, the results of AR are shown in Fig. 2 as the dashed curves. It must be pointed out that the dashed curve for the electrons was taken from Fig. 9 of Ref. 1. The dashed curve for the ions was obtained from Figs. 6 and 9 presented in the same reference. Consequently, there is some error as we present the data of AR which can be ascribed to taking information from their graphs. The calculations of AR were made for steady-state conditions and required that the electron and ion currents were equal throughout the discharge volume. For their case the equality of these currents is a necessity; however, for an afterglow there is no reason to expect this equality to hold. In fact, the electron and ion currents are not as a rule equal in the volume nor at the wall. This question of equality of currents in an afterglow was noted in

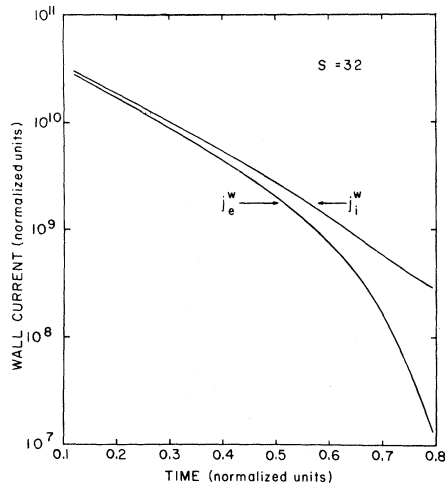


FIG. 3. The normalized electron and ion wall currents  $j_e^w$  and  $j_i^w$  as a function of normalized time for  $s=32$ .

Ref. 1. The electron and ion wall currents are shown in Fig. 3. It is only in the ambipolar limit that the electron and ion currents are approximately equal. From Fig. 2 it would appear that the AR theory adequately describes the approach to the transition in an afterglow, and apparently only at low electron densities (that is, in the approach to free diffusion) is there significant error in applying the results of Ref. 1 to an afterglow.

To quote from AR: "... a thermal plasma initial-

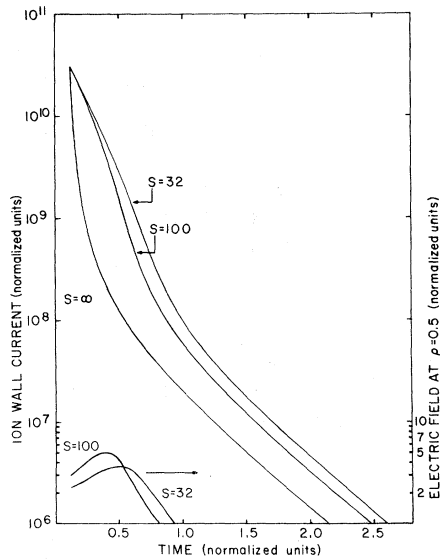


FIG. 4. The normalized ion wall current as a function of normalized time for  $s=32$ , 100, and  $\infty$ . Also shown are the normalized electric fields at  $\rho=0.5$  as a function of normalized time for  $s=32$  and 100.

ly situated on the curve will decay in a quasiequilibrium fashion closely following the curve." This statement refers to Fig. 2 and simply means that for an afterglow, regardless of initial conditions, exhibiting effective diffusion coefficients as given in Fig. 2 the decay will be described for all times into the successively later afterglow by Fig. 2. It is, of course, possible to have initial conditions such that the space-charge conditions do not satisfy the above "quasiequilibrium" conditions. In such a case, the charged particles will quickly adjust until they indeed follow the curves of Fig. 2.

The coefficient  $q=1.6$  in Fig. 2 represents the ratio of the maximum effective ion diffusion coefficient to the ambipolar diffusion coefficient. For  $s=100$ ,  $q$  has a value of 2.2. As  $s$  increases, the ions diffuse faster in the transition region relative to the ambipolar rate. The behavior of the ion transition as a function of  $s$  is shown in Fig. 4. As  $s$  increases, the electrons tend to leave the volume faster (thus at a higher ion density) with a resulting increase in the volume space-charge electric field which enhances the volume ion loss rate. The electric field at  $\rho=0.5$  shown in Fig. 4 illustrates this point. Figure 5 shows the effective ion diffusion coefficient as a function of  $P_0 \Lambda^2 \mu / D$ , where  $P_0$  is the central ion density. The dashed curves represent the behavior of the central ion density. The curve labeled  $s=\infty$  is the case where the electron density is identically zero everywhere and represents an upper bound to the effective ion diffusion coefficient. As  $s$  increases, the transition starts (this question of when the transition starts is really not sharply defined) at higher densities and still has the same asymptotic limit in free diffusion. As  $s$  gets larger, the transition lasts more decades of central electron and ion densities. In Fig. 5 note that towards the end of the transi-

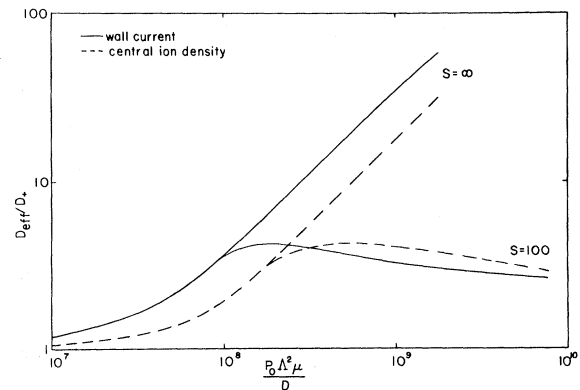


FIG. 5. The effective diffusion coefficient  $D_{eff}/D_*$  for the central ion density and the ion wall current as a function of  $P_0 \Lambda^2 \mu / D$  for  $s=100$  and  $\infty$ .

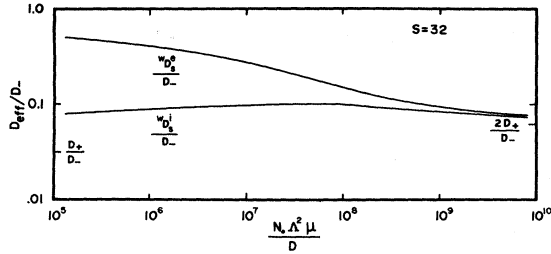


FIG. 6. The effective diffusion coefficient/ $D_0$  for the electron and ion wall currents as a function of  $N_0 A^2 \mu / D$  for  $s=32$ .

tion ( $P_0 A^2 \mu / D \lesssim 10^8$ ) the time dependence of the ions is the same for all  $s$ . This is because the electron density is so low that the self-field of the ions determines the ion decay rate.

One can define effective diffusion coefficients for the electron and ion wall currents by setting  $\rho=1$  in Eqs. (4a) and (4b) and replacing  $n$  and  $p$  by their respective wall currents. The coefficients are shown in Fig. 6 for  $s=32$ . The transition as seen on the wall currents lags that of the central densities, and the ion diffusion in the transition is slower on the ion wall current than in the central region.

Figure 7 shows the wall potential as a function of  $P_0 A^2 \mu / D$  for  $s=32$ , 100, and  $\infty$ . The upper bound to the wall potential is represented by the case of  $s=\infty$  and is just the potential due to the enclosed space charge (the positive ion density). As  $s$  is decreased, this space charge is offset by a finite electron density.

It is necessary to emphasize that only diffusion and the space-charge electric field have been considered in these calculations. In point of fact, there may be other relevant processes occurring such as recombination, negative ion formation, etc. For example, in a helium afterglow it is known that metastable atoms play an important role in deter-

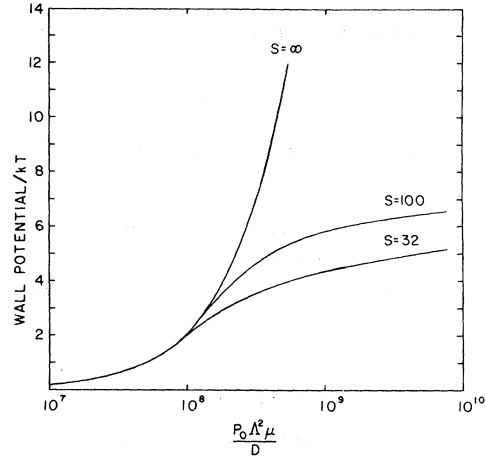


FIG. 7. The wall potential/ $kT$  as a function of  $P_0 A^2 \mu / D$  for  $s=32$ , 100, and  $\infty$ , where  $kT$  is in units of electron volts.

mining the afterglow decay in that they provide a source of free electrons via metastable-metastable collisions. If this source of free electrons is sufficiently large during the transition, then it might be expected that the rate of decay of the electrons and ions would be less than in the absence of this source (owing to a decreased space-charge electric field). That is to say, under the proper conditions one would expect the behavior of the transition to be governed to some degree by the metastable behavior.

In conclusion, the results of this work are calculations of the electron and ion behavior in an isothermal afterglow. These results are in qualitative agreement with the experiment of Gerber *et al.*<sup>4</sup> insofar as predicting the general features of the transition from electron-ion ambipolar diffusion to free diffusion. In addition, the results substantiate the general behavior predicted by the more elaborate steady-state calculations of Ref. 1.

\*Work supported by the U. S. Atomic Energy Commission.

<sup>1</sup>W. P. Allis and D. J. Rose, *Phys. Rev.* **93**, 84 (1954).

<sup>2</sup>R. J. Freilberg and L. A. Weaver, *Phys. Rev.* **170**, 336 (1968).

<sup>3</sup>H. W. Bandel and A. D. MacDonald, *J. Appl. Phys.* **40**, 4390 (1969).

<sup>4</sup>R. A. Gerber, M. A. Gusinow, and J. B. Gerardo, *Phys. Rev. A* **3**, 1703 (1971).

<sup>5</sup>I. M. Cohen and M. D. Kruskal, Princeton University Plasma Physics Laboratory Report No. MATT-202, 1963 (unpublished); a condensed version of this report

was published in *Phys. Fluids* **8**, 920 (1965).

<sup>6</sup>Mark D. Kregel, *J. Appl. Phys.* **41**, 1978 (1970).

<sup>7</sup>Erich S. Weibel, *Phys. Fluids* **10**, 741 (1967).

<sup>8</sup>E. H. Sondheimer, *Advan. Phys.* **1**, 1 (1952).

<sup>9</sup>Karl-Birger Persson, *Phys. Fluids* **5**, 1625 (1962).

<sup>10</sup>Z. Shimony and J. H. Cahn, *Phys. Fluids* **8**, 1704 (1965).

<sup>11</sup>J. Killeen and S. L. Rompel, Lawrence Radiation Laboratory Report No. UCRL-50-127, 1966 (unpublished).

<sup>12</sup>R. D. Richtmyer and K. W. Morton, *Difference Methods for Initial Value Problems*, 2nd ed. (Interscience, New York, 1967).